(19) Europäisches Patentamt
European Patent Office
Office européen des brevets

(11) EP 0 899 906 A2

(12) EUROPEAN PATENT APPLICATION

(43) Date of publication:
03.03.1999 Bulletin 1999/09

(51) Int Cl.[6]: **H04L 1/20**

(21) Application number: **98306614.3**

(22) Date of filing: **18.08.1998**

(84) Designated Contracting States:
AT BE CH CY DE DK ES FI FR GB GR IE IT LI LU MC NL PT SE
Designated Extension States:
AL LT LV MK RO SI

(30) Priority: **25.08.1997 US 921454**

(71) Applicant: **LUCENT TECHNOLOGIES INC.**
Murray Hill, New Jersey 07974-0636 (US)

(72) Inventors:
- **Balachandran, Krishna**
  Middletown, New Jersey 07748 (US)
- **Kadaba, Srinivas R.**
  Chatham, New Jersey 07928 (US)
- **Nanda, Sanjiv**
  Plainsboro, New Jersey 08536 (US)
- **Ejzak, Richard Paul**
  Wheaton, Illinois 60187 (US)

(74) Representative:
Buckley, Christopher Simon Thirsk et al
Lucent Technologies (UK) Ltd,
5 Mornington Road
Woodford Green, Essex IG8 0TU (GB)

(54) System and method for measuring channel quality information

(57) In a system and method to measure channel quality in terms of signal to noise ratio for the transmission of coded signals over fading channels, a Viterbi decoder metric for the Maximum Likelihood path is used as a channel quality measure. This Euclidean distance metric is filtered in order to smooth out short term variations. The filtered or averaged metric is a reliable channel quality measure which remains consistent across different coded modulation schemes and at different mobile speeds. The filtered metric is mapped to the signal to noise ratio per symbol using a threshold based scheme. Use of this implicit signal to noise ratio estimate is used for the mobile assisted handoff and data rate adaptation in the transmitter.

FIG. 11

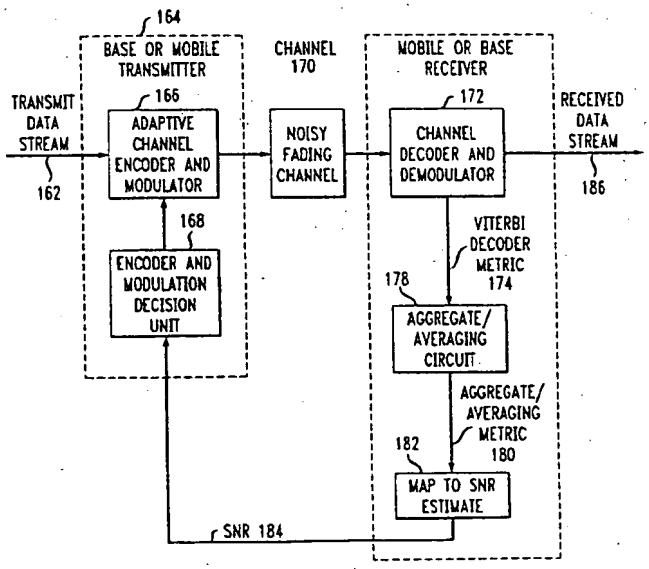

EP 0 899 906 A2

Description

BACKGROUND OF THE INVENTION

1. FIELD OF THE INVENTION

[0001] The present invention relates generally to the field of communication systems and, more particularly, to communications systems which measure the quality of channel information.

2. DESCRIPTION OF THE RELATED ART

[0002] As the use of wireless communications continues to grow worldwide at a rapid pace, the need for frequency spectrum efficient systems that accommodate both the expanding number of individual users and the new digital features and services such as facsimile, data transmission, and various call handling features has increased.

[0003] Current wireless data systems such as the cellular digital packet data (CDPD) system and the IS-130 circuit switched time division multiple access data system support only low fixed data rates which are insufficient for several applications. Becasue cellular systems are engineered to provide coverage at the cell boundary, the signal to interference plus noise ratio (SNR) over a large portion of a cell is sufficient to support higher data rates. Adaptive data rate schemes using bandwidth efficient coded modulation are currently have been proposed for increasing data throughput over the fading channels encountered in cellular systems. Increased data throughput is accomplished by using bandwidth efficient coded modulation schemes with higher information rates. However, a practical problem to using these schemes is to dynamically adjust the coded modulation to adapt to the channel conditions.

[0004] At present, there is a need to determine the channel quality based on the measurements or metrics of the SNR or the achievable frame error rate (FER) for the time varying channel. However, in cellular systems there is no fast accurate method to measure either the SNR or to estimate the FER.

[0005] The difficulty in obtaining these metrics in a cellular system is due to the time varying signal strength levels found on the cellular channel. The time varying signal strength levels, sometimes referred to as fading, are the result of the movement of the mobile station or cellular phone relative to the base station (also known as a cell site). Recent schemes propose a short term prediction of the FER, but not the SNR, using the metric for the second best path by a Viterbi decoder. This metric is computationally very intensive and reacts to short term variations in fading conditions. Therefore, there is a need, in the field of wireless communication systems, for a method accurately measuring the channel quality in terms of the SNR.

[0006] It is also important to measure channel quality, in terms of SNR or FER, for the purpose of mobile assisted handoff (MAHO). However, FER measurements are usually very slow for the purpose of handoff or rate adaptation. FER as a channel quality metric is slow because it can take a very long time for the mobile to count a sufficient number of frame errors. Therefore, there is a need for a robust short term channel quality indicator that can be related to the FER.

[0007] As a result, channel quality metrics such as symbol error rate, average bit error rate and received signal strength measurements have been proposed as alternatives. The IS-136 standard already specifies measurement procedures for both bit error rate and received signal strength. However, these measures do not correlate well with the FER, or the SNR, which is widely accepted as the meaningful performance measure in wireless systems. Also, received signal strength measurements are often inaccurate and unreliable. The present invention is directed to overcoming, or at least reducing the effects of one or more of the problems set forth above.

SUMMARY OF THE INVENTION

[0008] In accordance with one aspect of the present invention there is provided a system and method for determining the signal to noise ratio which provides for establishing a set of path metrics corresponding to a set of predetermined signal to noise ratios. A digital signal is received and a path metric determined for the digital signal. Mapping of the path metric is provided to a corresponding signal to noise ratio in the set of predetermined signal to noise ratios.

[0009] These and other features and advantages of the present invention will become apparent from the following detailed description, the accompanying drawings and the appended claims.

BRIEF DESCRIPTION OF THE DRAWINGS

[0010] The advantages of this invention will become apparent upon reading the following detailed description and upon reference to the drawings in which:

FIG. 1 is a graphical representation of three cell sites within a cluster;

FIG. 2 is a block diagram of both the base station and the mobile station transmitters and receivers for the present invention;

FIG. 3 is a block diagram of a decoder system for present invention;

FIG. 4 is a graph having a curve, with the vertical scale representing the average Viterbi decoder metric and the horizontal scale representing the time slot pair (block) number;

FIG. 5 is a graph having a curve, with the vertical scale representing the average Viterbi decoder metric and the horizontal scale representing the SNR;

FIG. 6 is a flow diagram illustrating the steps performed during the process of determining the SNR using the lookup table and adjusting the coded modulation scheme used by the system;

FIG. 7 is a flow diagram illustrating the steps performed during the process of determining the SNR using the linear prediction and adjusting the coded modulation scheme used by the system;

FIG. 8 is a graph having a three curves, with the vertical scale representing the $\overline{FER}$ and the horizontal scale representing the SNR;

FIG. 9 is a table of values for a conservative mode adaptation strategy based on a Viterbi algorithm metric average;

FIG. 10 is a table of values for an aggressive mode adaptation strategy based on a Viterbi algorithm metric average;

FIG. 11 is a block diagram of both the base station and the mobile station transmitters and receivers for the implementation of an adaptive coding scheme; and

FIG. 12 is a block diagram of both the base station and the mobile station transmitters and receivers for the implementation of a mobile handoff scheme.

DETAILED DESCRIPTION

[0011] Referring to the drawings and initially to FIG. 1, a plurality of cells 2, 4, and 6 in a telecommunications system are shown. Consistent with convention, each cell 2, 4, and 6 is shown having a hexagonal cell boundary. Within each cell 2, 4, and 6 are base stations 8, 10, and 12 that are located near the center of the corresponding cell 2, 4, and 6. Specifically, the base station 8 is located within cell 2, base station 10 is located within cell 4, and base station 12 is located within cell 6.

[0012] The boundaries 14, 16 and 18 separating the cells 2, 4, and 6 generally represent the points where mobile assisted handoff occurs. As an example, when a mobile station 20 moves away from base station 8 towards an adjacent base station 10, the SNR from the base station 8 will drop below a certain threshold level past the boundary 14 while, at the same time, the SNR from the second base station 10 increases above this threshold as the mobile station 20 crosses the boundary 14 into cell 4. Cellular systems are engineered to provide coverage from each base station up until the cell boundary. Thus, the SNR over a large portion of a cell 2 is sufficient to support higher data rates because the SNR from the base station 8 is greater than the minimum SNR needed to support the data transfer at the boundary 14. FIG. 2 is an example implementation of an adaptive rate system which takes advantage of this support for higher data rates.

[0013] FIG. 2 is a block diagram for the schematic of the base station 8 and the mobile station 20 for the invention. The base station 8 consists of both an adaptive rate base station transmitter 22 and an adaptive rate base station receiver 24. Likewise, the mobile station 20 also consists of both an adaptive rate mobile station receiver 26 and an adaptive rate mobile transmitter 28. Each pair of the transmitter and the receiver, corresponding to either the base station 8 or mobile station 20, are in radio connection via a corresponding channel. Thus, the adaptive rate base station transmitter 22 is connected through a downlink radio channel 30 to the adaptive rate mobile receiver 26 and the adaptive rate mobile station transmitter 28 is connected through an uplink radio channel 32 to the adaptive rate base station receiver 24. This implementation allows for increased throughput between the base station 8 and the mobile station 20 over both the downlink channel 30 and the uplink channel 32 because of the use of adaptive bandwidth efficient coded modulation schemes.

[0014] Thus, the information rate may be varied by transmitting at a fixed symbol rate (as in IS-130/IS-136), and changing the bandwidth efficiency (number of information bits per symbol) using a choice of coded modulation schemes.

However, coded modulation schemes with different bandwidth efficiencies have different error rate performance for the same SNR per symbol. At each SNR, the coded modulation scheme is chosen which results in the highest throughput with acceptable FER and retransmission delay. Therefore, detection of channel quality in terms of SNR or achievable FER is very important for this invention. Both the SNR and FER as channel quality metrics can be derived from the cumulative Euclidean distance metric corresponding to a decoded received sequence.

[0015] A block diagram of a encoder and decoder system for the invention is shown in FIG. 3. Within the transmitter 34, the information sequence (a_k) 36 is encoded using a convolutional encoder 38 to provide a coded sequence $\{b_k\}$ 40. The coded sequence $\{b_k\}$ 40 is then mapped through a symbol mapper 42 to a symbol $\{s_k\}$ 44 from either an M-ary constellation such as M-ary phase shift keying (PSK) or a M-ary quadrature amplitude modulation (QAM) scheme using either a straightforward Gray mapping or a set partitioning technique. Pulseshaping is then carried out using transmit filters 46 that satisfy the Gibby Smith constraints (i.e. necessary and sufficient conditions for zero intersymbol interference). The symbol $\{s_k\}$ 44 is then transmitted through the channel 48 to the receiver 50. At the receiver 50, the front end analog receive filters 52 are assumed to be matched to the transmit filters 46 and the output $\{r_k\}$ 54 is sampled at the optimum sampling instants.

[0016] The received symbol at the k^{th} instant is given by

$$r_k = \alpha_k s_k + n_k,$$

where s_k denotes the complex transmitted symbol $\{s_k\}$ 44, α_k represents the complex fading channel 64 coefficient and $\bar{n}_k$ denotes the complex additive white Gaussian noise (AWGN) with variance N_o. For this example, the fading channel 64 is assumed to be correlated, and may be represented by a number of models. In this example the Jakes' model for Rayleigh fading is used. The convolutional encoder 38 is chosen to optimize the systems needs. Here, a trellis code has been chosen, however, many other codes could also be used by this invention without modifying the essence of the invention. Maximum likelihood decoding at the receiver 50 may be carried out using a Viterbi algorithm circuit (also known as a maximum likelihood decoder) 56 to search for the best path through a trellis. An estimate of the complex fading channel 64 coefficients is assumed available to the decoder (i.e. the convolutional encoder 58) of the receiver 50.

[0017] The Viterbi algorithm circuit 56 associates an incremental Euclidean distance metric with each trellis branch transition and tries to find the transmitted sequence (s_k) 44 that is closest in Euclidean distance to the received sequence $\{r_k\}$ 54. The Viterbi algorithm circuit 56 processes each possible data sequence $\{\underline{\sigma_i}\}$ through both a convolutional encoder 58 and symbol mapper 60 to produce a possible decoded sequence decoded sequence $\{\underline{\hat{s}_i}\}$ 62. The Viterbi algorithm circuit 56 then uses the received sequence $\{r_k\}$ 54 and the estimated channel coefficient $\{a_k\}$ 64 in an incremental Euclidean distance metric computation circuit 66 which computes the incremental Euclidean distance. The incremental Euclidean distance metric is then processed through a cumulative feedback loop 68 which produces the cumulative path metric 72. Next, the cumulative path metric 72 and the cumulative metrics corresponding to all possible transmitted sequences $\{\underline{\sigma_i}\}$ 70 are input into a minimum metric processor circuit 74 which outputs both the decoded data sequence $\{\underline{\hat{c}_i}\}$ 76 and the minimum metric m_i for the i^{th} block. The cumulative path metric corresponding to the decoded sequence $\{\underline{\hat{s}_i}\}$62 is given by

$$m_i = \min_{\hat{s}_k} \sum_{k=0}^{N-1} |r_k - \alpha_k \hat{s}_k|^2$$

where α_k 64 is the estimated fading channel coefficient at the k^{th} instant, and the trellis is assumed to terminate at a known state after every N symbols.

[0018] Thus, in accordance with one aspect of the present invention, the Viterbi decoder is used to derive the channel quality information from the cumulative Euclidean distance metric corresponding to the decoded trellis path for each block. However, as noted earlier, the Euclidean distance metric has large variations from one block to another in the presence of a fading channel. Thus smoothing, such as averaging, of these variation is required to obtain a good estimate of the metric. A small cumulative Euclidean distance metric would indicate that the received sequence is very close to the decoded sequence. For well designed trellis codes, this situation would only occur under good channel conditions with high SNR. Under poor channel conditions, the metric is much higher. Thus, a good estimate of the metric can be obtained at the i^{th} block of N symbols by using the following relationship:

$$M_i = \alpha M_{i-1} + (1 - \alpha) m_i,$$

for α greater than zero and less than 1.0, where m_i represents the decoded trellis path metric and a represents the filter coefficient which determines the variance of the estimate.

[0019] FIG. 4, illustrates a graph having a four curves, with the vertical scale representing the average Viterbi decoder metric M_i and the horizontal scale representing the block number. The solid line curves 80 - 86 represent the time evolution of the filtered Viterbi decoder metric for a trellis coded 8 PSK scheme and a filter coefficient α equal to 0.9. An IS-130/IS-136 time slot structure (N = 260 symbols) is assumed and the trellis is terminated at the end of each time slot pair. The SNR ranges from 30 dB to 16 dB and is decremented in steps of 2 dB after every 600 time slot pairs. Each solid line curve represents a different combination of f_d, the doppler frequency, multiplied by T, the symbol duration. Therefore, the solid line curve parameters are as follows: *(a)* $f_dT = 0.0002$ for solid line curve 80; *(a)* $f_dT = 0.0012$ for solid line curve 82; *(a)* $f_dT = 0.0034$ for solid line curve 84; and *(a)* $f_dT = 0.0069$ for solid line curve 86. From FIG. 4, it is clear that there exists a straightforward one to one mapping between the average Euclidean distance metric M_i and the SNR. It maintains a steady level when the SNR is fixed and increases when the SNR decreases.

[0020] FIG. 5 shows a graph having four curves, with the vertical scale representing the long term average Viterbi decoder metric μ (the expected value of M_i) and the horizontal scale representing the SNR. Again, as in FIG. 4, the four curves 88 - 94 represent different doppler frequencies. From FIG. 5, it is clear that the average metric μ does not depend on the mobile speed. As a result, the long term cumulative metric average, μ, is the target metric for the present invention. Thus, once the Euclidean metric has been obtained it can be either mapped to the corresponding SNR in a lookup table or through a linear prediction approach.

[0021] The long term cumulative metric average μ and the SNR satisfy the empirical relationship

$$SNR = 10\log_{10}\frac{NE_s}{\mu} \text{ in dB},$$

where E_s is the average energy per transmitted symbol and N is the number of symbols per block. This behavior remains identical across the different coded modulation schemes. Therefore, the average Viterbi decoder metric provides a very good indication of the SNR. Furthermore, the short term average of the metric may be determined using the above mentioned relationship $M_i = \alpha M_{i-1} + (1 - \alpha) m_i$. FIG. 4 shows that the short term average satisfies

$$\theta_{low} < \frac{M_i}{\mu} < \vartheta_{high}$$

where the target metric, μ, is obtained from

$$SNR = 10\log_{10}\frac{NE_s}{\mu}.$$

The thresholds, θ_{low} and θ_{high} depend on the standard deviation of M_i which, in turn, is a function of the filter parameter, α. Thus, the present invention incorporates two possible ways to determine the SNR from the average metric M_i.

[0022] FIG. 6 is a flow diagram describing the steps performed by either the base station or the mobile station in determining the SNR from the average metric M_i using a lookup table. The process begins in step 88 in which the cellular network determines the SNR range of interest. This SNR range is determined by the needs of the network at any given time.

[0023] The next step 98 is to generate a table of target values μ_n in descending order of SNR for the determined range of interest. Arrangement in descending order is purely for example and not a necessary or limiting aspect of the process. The target values are determined by the following relationship

$$\mu_n = \frac{NE_s}{10^{0.1(SNR_n)}}$$

for $n = 1, 2, \ldots K$, where K determines the desired granularity. In step 100, these values of μ_n versus the corresponding value of SNR are then stored into a memory unit for later use in mapping the measured values of $\frac{M_i}{\mu_n}$ to the corresponding

SNR values in the lookup table. Once the process of creating and storing the lookup table of μ_n versus SNR_n is complete, the system is then ready to receive and transmit data information.

[0024] In step 102, the receiver receives, for this example, a trellis coded signal and then decodes the received coded signal and outputs the trellis path metric m_i in step 104. For this example, the system uses a Viterbi Minimum Likelihood decoder to determine the trellis path metric m_i. Once the trellis path metric m_i is determined the system then determines M_i, the average metric for the i^{th} block, in step 106 using the relationship $M_i = \alpha M_{i-1} + (1 - \alpha)m_i$.

[0025] The process continues to decision step 108 in which a threshold detector circuit determines whether the value $\frac{M_i}{\mu_1}$ is less than the predetermined threshold θ_{low}. If the outcome of the decision step 108 is a "YES" determination, the process continues to step 110. In step 110, the system recognizes that the measured SNR is greater than the SNR_1 (the maximum SNR for the range of the lookup table). As a result, the system in step 110 clips the measured SNR to be equal to SNR_1. Next, the system in step 112 provides the SNR value SNR_1 to the transmitter.

[0026] If the outcome of the determination step 108 is a "NO" determination, the process continues instead to decision step 114 in which a second threshold detector circuit determines whether the value $\frac{M_i}{\mu_k}$ is greater than the predetermined threshold θ_{high}. If the outcome of the decision step 114 is a "YES" determination, the process continues to step 116. In step 116, the system recognizes that the measured SNR is less than the SNR_k (the minimum SNR for the range of the lookup table). As a result, the system in step 116 clips the measured SNR to be equal to the SNR_k. Next, the system in step 112 provides the SNR value SNRk to the transmitter.

[0027] If, on the other hand, the outcome of the determination step 114 is a "NO" determination, the process continues instead to decision step 118 in which a threshold detector circuit determines the threshold μ_n for which the value $\frac{M_i}{\mu_n}$ is both less than the predetermined threshold θ_{high} and greater than the predetermined threshold θ_{low}. The system in step 120 sets the measured SNR equal to the corresponding SNR_n for the mapped value of $\frac{M_i}{\mu_n}$ in the lookup table. As a result, the system in step 112 provides the SNR value SNR_n to the transmitter.

[0028] FIG. 7 is a flow diagram describing the steps performed by either the base station or the mobile station in determining the SNR from the average metric M, using a linear prediction process. The process begins in step 126 in which the cellular network determines the SNR range of interest. Similar to the lookup table approach describe earlier, this SNR range is first determined by the needs of the network at any given time. However, the use of a linear prediction, instead of the direct mapping of a lookup table, approach allows the receiver to react faster to the changes of SNR within the cell.

[0029] In step 126, a table of target values μ_n, in descending order of SNR, is generated for the determined range of interest. Again, arrangement in descending order is purely for example and not a necessary or limiting aspect of the process. The target values are determined by the following relationship

$$\mu_n = \frac{NE_s}{10^{0.1(SNR_n)}}$$

for $n = 1, 2, \ldots K$, where K determines the desired granularity. In step 128, these values of μ_n versus the corresponding value of the SNR are then stored into a first memory unit for later use in mapping the measured values of $\frac{M_i}{\mu_n}$ to the corresponding SNR values in the lookup table. Once the process of creating and storing the lookup table of μ_n versus SNR_n is complete, the system is then ready to receive and transmit data information.

[0030] In step 130, the receiver receives a coded signal, a trellis code for the example, and then decodes the received coded signal and outputs the trellis path metric m_i in step 132. Again, for this example, the system uses a Viterbi Minimum Likelihood decoder to determine the trellis path metric m_i. Once the trellis path metric m_i is determined, the system then determines M_i the average metric for the i^{th} block in step 134 using the relationship $M_i = \alpha M_{i-1} + (1 - \alpha) m_i$. Then in step 136, the values of an optimal p^{th} order linear predictor h_l (for $l = 0, 1, \ldots, p-1$) are generate and stored in to a second memory unit for later use. Next, in step 138, the process proceeds and determines the future value of $\tilde{M}_{i+D}$ from the previous values of $\tilde{M}_{i-p}$ using the relation

$$\tilde{M}_{i+D} = \sum_{l=0}^{p-1} h_l M_{i-l}$$

[0031] The process continues to decision step 140 in which a threshold detector circuit determines whether the value

$$\frac{\tilde{M}_{i+D}}{\mu_l}$$

is less than the predetermined threshold θ_{low}. If the outcome of the decision step 140 is a "YES" determination, the process continues to step 142. The system in step 142 clips the measured SNR to be equal to SNR_1. Next, the system in step 144 provides the SNR value SNR_1 to the transmitter.

[0032] If the outcome of the determination step 140 is a "NO" determination, the process continues instead to decision step 146 in which a second threshold detector circuit determines whether the value

$$\frac{\tilde{M}_{i+D}}{\mu_k}$$

is greater than the predetermined threshold θ_{high}. If the outcome of the decision step 146 is a "YES" determination, the process continues to step 148. The system in step 148 clips the measured SNR to be equal to SNRk. Next, the system in step 144 provides the SNR value SNR_k to the transmitter.

[0033] If, on the other hand, the outcome of the determination step 146 is a "NO" determination, the process continues instead to decision step 150 in which a threshold detector circuit determines whether the value

$$\frac{\tilde{M}_{i+D}}{\mu_n}$$

is both less than the predetermined threshold θ_{high} and greater than the predetermined threshold θ_{low}. The system in step 152 sets the measured SNR equal to the corresponding SNR_n for the mapped value of

$$\frac{\tilde{M}_{i+D}}{\mu_n}$$

in the lookup table. As a result, the system in step 144 provides the SNR value SNR_n to the transmitter.

[0034] This linear prediction approach helps the receiver use the current value and *p-1* past values of the average metric to predict the channel quality metric *D* blocks in the future. Thus, this allows the receiver to react quickly to changes in the SNR.

[0035] While SNR is the preferred performance measure in the present invention, it is well known that performance is often measured in terms of FER for the forward and reverse links. At a fixed SNR, the FER may often be different at different mobile speeds. In order to obtain a FER indication the SNR should be mapped to the average FER under some wide range of mobility. At each value of SNR, define the weighted sum

$$\overline{FER} = \sum_i f_i w_i$$

where $\Sigma w_i = 1$, f_i is the FER at speed, v_i, the coefficient, w_i, represents the weight assigned to the speed and $\overline{FER}$ denotes the weighted average FER. By this technique it is possible to use the average metric to determine the SNR which in turn may be mapped to $\overline{FER}$.

[0036] As an example of an implemented rate adaptation system using the SNR measurements as a channel quality indicator. Let C_1, C_2, ..., C_Q represent, in ascending order of bandwidth efficiency, the *Q* different modes of operation schemes for the transmitter. These different schemes may be implemented by using a fixed symbol rate and changing the trellis encoder and symbol mapper to pack a variable number of information bits per symbol. The upper bound on achievable throughput for each C_j at some SNR is given by $\underline{R(C_j)(1-\overline{FER}(C_j,SNR))}$ where $R(C_j)$ is the data rate corresponding to C_j in bits/second. The actual throughput can be lower as it also depends on higher recovery layers which

may time-out during retransmission.

[0037] FIG. 8, illustrates a graph having a three curves, with the vertical scale representing the $\overline{FER}$ and the horizontal scale representing the SNR. The curves 154, 156, and 158 represent three hypothetical coded modulation schemes. For each coded modulation scheme, C_j, $\overline{FER}_j$ is the average FER averaged over mobile speeds. As an example, associated with curve 156 is adaptation point A_j 160. If the SNR falls below this point the transmitter must change its mode from scheme C_j to scheme C_{j-1} and begin operation on curve 154, at B_{j-1} 155, corresponding to scheme C_{j-1}, above which C_j has lower throughput than C_{j-1}. The filtered Viterbi decoder metric may be used as an indicator of SNR at the mode adaptation point. For the i^{th} decoded block, set $M_i=\underline{M_i}$ or $M_i=\underline{M_{i-1}}$ depending on the choice of filter parameter.

[0038] θ_{high} and θ_{low} are the thresholds which depend on the filter parameter, α. Then, the adaptation rule for the data transmission is as follows: After the i^{th} block, if the transmitter is currently operating with C_j change the mode of operation to

$$C_{j-1}, \text{ if } \underline{M_i} / \mu_j > \theta_{high}, \text{ for } j = 2, 3, \ldots, Q$$

and

$$C_{j+1}, \text{ if } \underline{M_i} / \mu_{j+r} < \theta_{low}, \text{ for } j = 1, 2, \ldots, Q - 1$$

where r = 1, 2, ..., $Q - j$. For each j, the highest allowable value of r maximizes the throughput by permitting a operation at a higher rate in bits per symbol. Finally, filtering of the metric can be applied across the coded modulation schemes since the metric average, μ, is independent of the mobile speed or the coded modulation scheme. Thus, there is no need to reset the channel quality measure after the adaptation.

[0039] Applying actual data to this example, FIG. 9 shows a table of values for a conservative mode adaptation strategy based on a Viterbi algorithm metric average. In, FIG. 9, C_1, C_2, and C_3 represent three coded modulation schemes where the choice of C_1 results in the lowest data rate and C_3 results in the highest data rate. Here, μ_1, μ_2 and μ_3 are the target metrics corresponding to the $\overline{FER}$ adaptation points for the three respective coded modulations. The thresholds θ_{high} and θ_{low} are defined such that θ_{high} is greater than 1.0 and θ_{low} less than 1.0. Additionally, FIG. 10 show a table of values for a aggressive mode adaptation strategy based on a Viterbi algorithm metric average.

[0040] A block diagram of an adaptive rate system for the invention is shown in FIG. 11. The diagram shows the possible implementation of the system at either the base station or the mobile station The system operates in the following way. Initially, the system organizes the information to be transmitted into a transmit data stream 162. The transmit data stream 162 is then input into the transmitter 164 of the system. Within the transmitter 164, the transmit data stream 162 is encoded and modulated by the adaptive channel encoder and modulator 166. The encoding and modulation employed by the adaptive channel encoder and modulator 166 is controlled by the encoder and modulation decision unit 168. The encoder and modulation decision unit 168 determines the correct encoding and modulation scheme in response to the received SNR estimate 184 from the receiver 172. Initially, the encoder and modulation decision unit 168 chooses a predetermined scheme which is input to the adaptive channel encoder and modulator 166. The adaptive channel encoder and modulator 166 then encodes and modulates the transmit data stream 162 to a predetermined scheme and transmits the information through a channel 170 (possibly noisy and fading) to the receiver 172. After the information is received at the receiver 172 it is input into a channel decoder and demodulator 174 which produces two outputs. The first output of the channel decoder and demodulator 174 is a value of the Viterbi decoder metric 176 for the received information signal. The second output of the channel decoder and demodulator 174 is the received data stream 186 which will be the same as the information sent by the transmit data stream 162 a large fraction of the time. Next, the value of the Viterbi decoder metric 176 is averaged by an aggregate/averaging circuit 178 producing a moving average value for the Viterbi decoder metric 180. The moving average value for the Viterbi decoder metric 180 is then mapped to SNR estimate 184 by a mapping circuit 182. The resulting SNR estimate 184 is fed back into the encoder and modulation decision unit 168 to determine the encoder and modulation scheme to be used corresponding to the SNR estimate 184. The new scheme value of the encoder and modulation decision unit 168 is input into the adaptive channel encoder and modulator 166 which switches to the new encoding and modulation scheme for the transmit data stream 162 and transmits the information over the channel 170.

[0041] A block diagram of a system using the SNR to do power control is shown in FIG. 12. The diagram shows the possible implementation of the system at either the base station or the mobile station. The system operates in the following way. Initially, the system organizes the information to be transmitted into a transmit data stream 188. The transmit data stream 188 is then input into the transmitter 190 of the system. Within the transmitter 190, the transmit data stream 188 is encoded and modulated by the channel encoder and modulator 192. The transmit power level at

the channel encoder and modulator 192 is controlled by the power control algorithm circuit 212. The power control algorithm circuit 212 may determine the power control level in response to the received SNR estimate 210 from the receiver 196. Additionally, the power control algorithm circuit 212 may also determines the power control level in response to the signal strength and bit error rate estimate 200 from the receiver 196. Initially, the power control algorithm circuit 212 is set to a predetermined value which is input to the channel encoder and modulator 192. The channel encoder and modulator 192 then encodes and modulates the transmit data stream 188 using a predetermined encodes and modulation scheme and transmits the information at a predetermined power level through a channel 194 (possibly noisy and fading) to the receiver 196. After the information is received at the receiver 196 it is input into a channel decoder and demodulator 198 which produces three outputs. The first output of the channel decoder and demodulator 198 is a value of the Viterbi decoder metric 202 for the received information signal. The second output is estimates of the signal strength and bit error rate 200. The third output of the channel decoder and demodulator 198 is the received data stream 218 which should be the same as information sent by the transmit data stream 188. Next, the value of the Viterbi decoder metric 202 is averaged by an aggregate/averaging circuit 204 producing an average value for the Viterbi decoder metric 206. The average value for the Viterbi decoder metric 206 is then mapped to SNR estimate 210 by a mapping circuit 208. The resulting SNR estimate 210 is fed back into the power control algorithm circuit 212 to determine a power control value corresponding to the SNR estimate 210. The new power control value of the power control algorithm circuit 212 is input into the channel encoder and modulator 192 for use in subsequent transmissions of the data stream 188 over the channel 194 to the receiver.

[0042] Additionally, the mobile assisted handoff decision circuit 214 also processes the SNR estimate 210 and the signal strength and bit error rate estimates 200. If the SNR value is below a predetermined threshold the mobile assisted handoff decision circuit 214 sends a message to the handoff processor 216 to handoff the mobile station to a new base station.

[0043] In conclusion, the following summary should easily enable one skilled in the art to practice the invention. The first part of the invention is an apparatus for adaptively changing the modulation schemes of a transmit data stream based on the measured SNR of a channel. The adaptive modulation schemes are implemented in a transmitter by an adaptive channel encoder and modulator. An encoder and modulation decision unit is connected to the transmitter adaptive channel encoder and modulator to determine the correct encoding and modulation scheme based on the information received at the receiver. Then a receiver channel decoder and demodulator is placed in radio connection with the transmitter adaptive channel decoder and demodulator through the channel. This transmitter adaptive channel decoder and demodulator produces a path metric value which is averaged by an averaging circuit to produce an averaged path metric value. This averaged path metric value is then mapped through a mapping device to a SNR estimate value. The SNR estimate value is then input into the transmitter encoder and modulation decision unit to determine if the coding and modulation scheme should be changed in response to the SNR estimate value. It should be noted that the receiver channel decoder and modulator may be implemented in various way, however, in this example implementation a Viterbi decoder was used.

[0044] The second part of the invention is an apparatus for implementing mobile assisted handoff based on the measured SNR of a channel. The mobile assisted hand off is implemented in a transmitter by a channel encoder and modulator. A receiver channel decoder and demodulator is in radio connection with the transmitter channel decoder and demodulator through a channel. The receiver channel decoder and demodulator produces a path metric value in response to the information received by the receiver which is averaged by an averaging circuit to produce an averaged path metric value. This averaged path metric value is then mapped through a mapping device to a SNR estimate value. A power control algorithm circuit is connected to the transmitter channel encoder and modulator which varies the power level of the transmitter in response to the SNR estimate value. Finally, the SNR estimate value is input into a mobile assisted handoff decision unit which determines if the mobile station should perform a handoff operation based on the SNR estimate value. As in the first part of the invention, it should again be noted that the receiver channel decoder and modulator may be implemented in various way, however, in this example implementation a Viterbi decoder was used. Additionally, this second part of the invention can be either implement at the mobile station or the base station.

[0045] Please note that while the specification in this invention is described in relation to certain implementations or embodiments, many details are set forth for the purpose of illustration. Thus, the foregoing merely illustrates the principles of the invention. For example, this invention may have other specific forms without departing from its spirit or essential characteristics. The described arrangements are illustrative and not restrictive. To those skilled in the art, the invention is susceptible to additional implementations or embodiments and certain of the details described in this application can be varied considerably without departing from the basic principles of the invention. It will thus be appreciated that those skilled in the art will be able to devise various arrangements which, although not explicitly described or shown herein, embody the principles of the invention and are thus within its spirit and scope. The scope of the invention is indicated by the attached claims.

Claims

1. A method for determining the signal to noise ratio, comprising the steps of:

establishing a set of path metrics corresponding to a set of predetermined signal to noise ratios;

receiving a digital signal;

determining a path metric for said digital signal; and

mapping said path metric to said corresponding signal to noise ratio in said set of predetermined signal noise to ratios.

2. The method of claim 1, wherein said digital signal is a coded signal.

3. The method of claim 1 wherein said digital signal is a trellis coded signal.

4. The method of claim 1 wherein the step of determining a path metric for said digital signal, further comprises the steps of:

establishing a set of signal to noise ratio values corresponding to a set of predetermined short term average of metric values, said short term average of metric values defined as M_i/μ;

determining a decoded path metric from said received digital signal using a decoder, said decoded path metric defined as m_i;

averaging m_i; and

storing in a second memory unit said average decoded path metric, said average decoded path metric defined as μ; and

determining an estimated Euclidean distance metric.

5. The method of claim 5 wherein the step of determining the estimated Euclidean distance metric is performed using the following equation:

$$M_i = \alpha M_{i-1} + (1-\alpha)\, m_i$$

where said estimated Euclidean distance metric is defined as M_i and α is a predetermined filter coefficient which is greater than zero and less than 1.0.

6. The method of claim 5 including the steps of:

determining a standard deviation *of* M_i;

determining average metric thresholds defined as θ_{low} and θ_{high} based on said standard deviation *of* M_i;

determining a value for M_i/μ by dividing said value of M_i by said value of μ;

mapping said value of M_i/μ to a minimum value of said corresponding signal to noise ratio *if* M_i/μ is less than θ_{low};

mapping said value *of* M_i/μ to a maximum value of said corresponding signal to noise ratio *if* M_i/μ is greater than θ_{high}; and

mapping said value of M_i/μ to said corresponding signal to noise ratio.

7. The method of claim 4 wherein said decoder is a Viterbi decoder for the maximum likelihood path.

8. A system for determining the signal to noise ratio, comprising:

means for establishing a set of path metrics corresponding to a set of predetermined signal to noise ratios;

means for receiving a digital signal;

means for determining a path metric for said digital signal; and

means for mapping said path metric to said corresponding signal to noise ratio in said set of predetermined signal noise to ratios.

9. The system of claim 1, wherein said digital signal is a coded signal.

10. The system of claim 1 wherein said digital signal is a trellis coded signal.

11. The system of claim 8 wherein the step of determining a path metric for said digital signal, further comprises:

means for establishing a set of signal to noise ratio values corresponding to a set of predetermined short term average of metric values, said short term average of metric values defined as M/μ;

means for determining a decoded path metric from said received digital signal using a decoder, said decoded path metric defined as m_i;

means for averaging m_i; and

means for storing in a second memory unit said average decoded path metric, said average decoded path metric defined as μ; and

means for determining an estimated Euclidean distance metric.

12. The system of claim 5 wherein the means for determining the estimated Euclidean distance metric is performed using the following equation:

$$M_i = \alpha M_{i-1} + (1-\alpha)\, m_i$$

where said estimated Euclidean distance metric is defined as M_i and α is a predetermined filter coefficient which is greater than zero and less than 1.0.

13. The system of claim 12 including the steps of:

means for determining a standard deviation *of* M_i;

means for determining average metric thresholds defined as θ_{low} and θ_{high} based on said standard deviation *of* M_i;

means for determining a value for M/μ by dividing said value *of* M_i by said value of μ;

means for mapping said value of M/μ to a minimum value of said corresponding signal to noise ratio in said lookup table if M/μ is less than θ_{low};

means for mapping said value of M/μ to a maximum value of said corresponding signal to noise ratio in said lookup table if M/μ is greater than θ_{high}, and

means for mapping said value *of* M/μ to said corresponding signal to noise ratio.

14. The system of claim 4 wherein said decoder is a Viterbi decoder for the maximum likelihood path.

FIG. 1
PRIOR ART

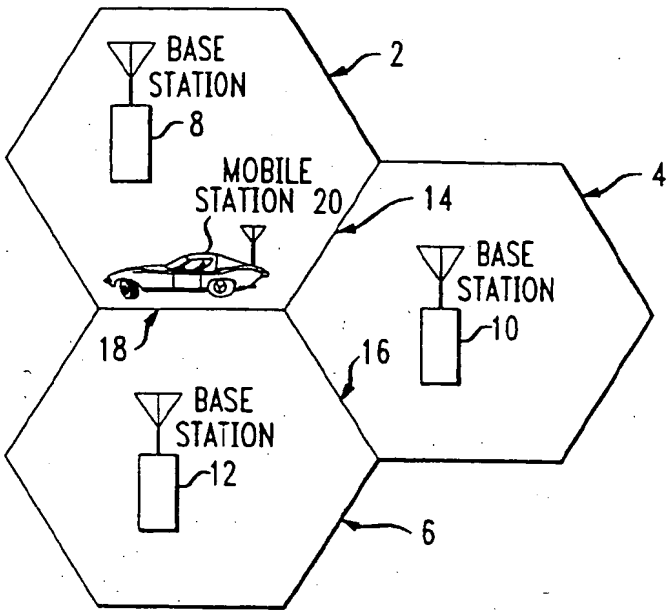

FIG. 2
PRIOR ART

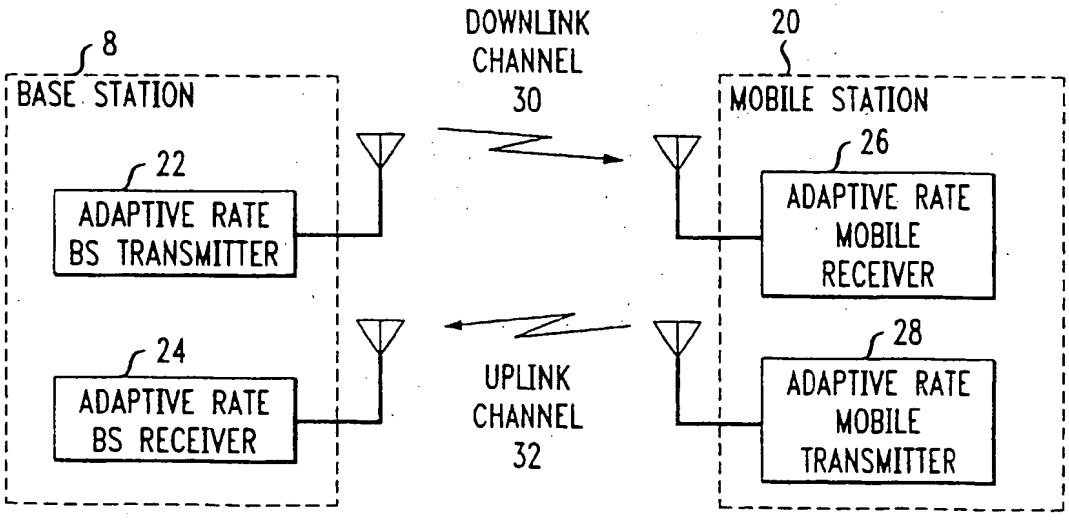

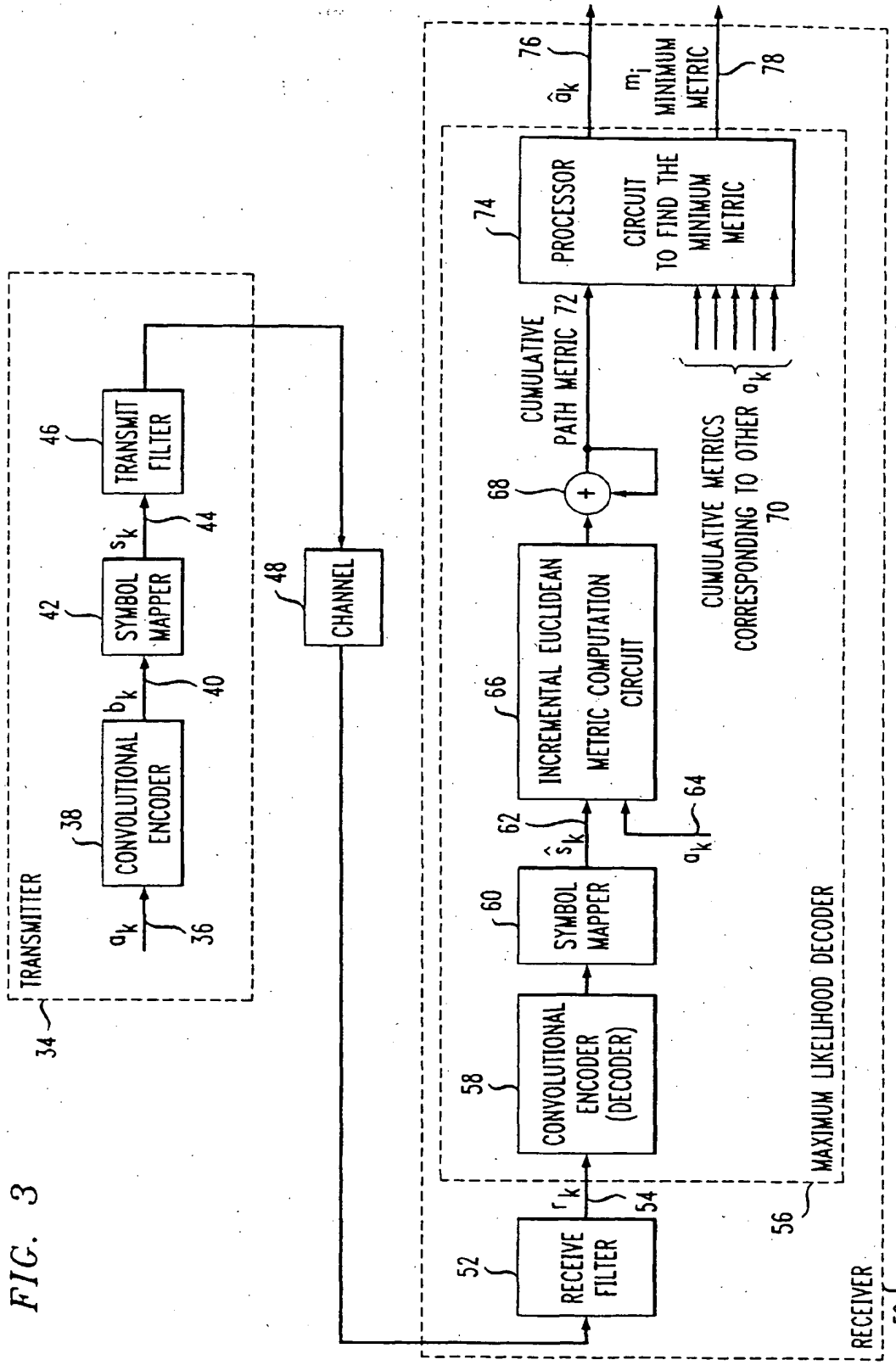

FIG. 3

FIG. 4

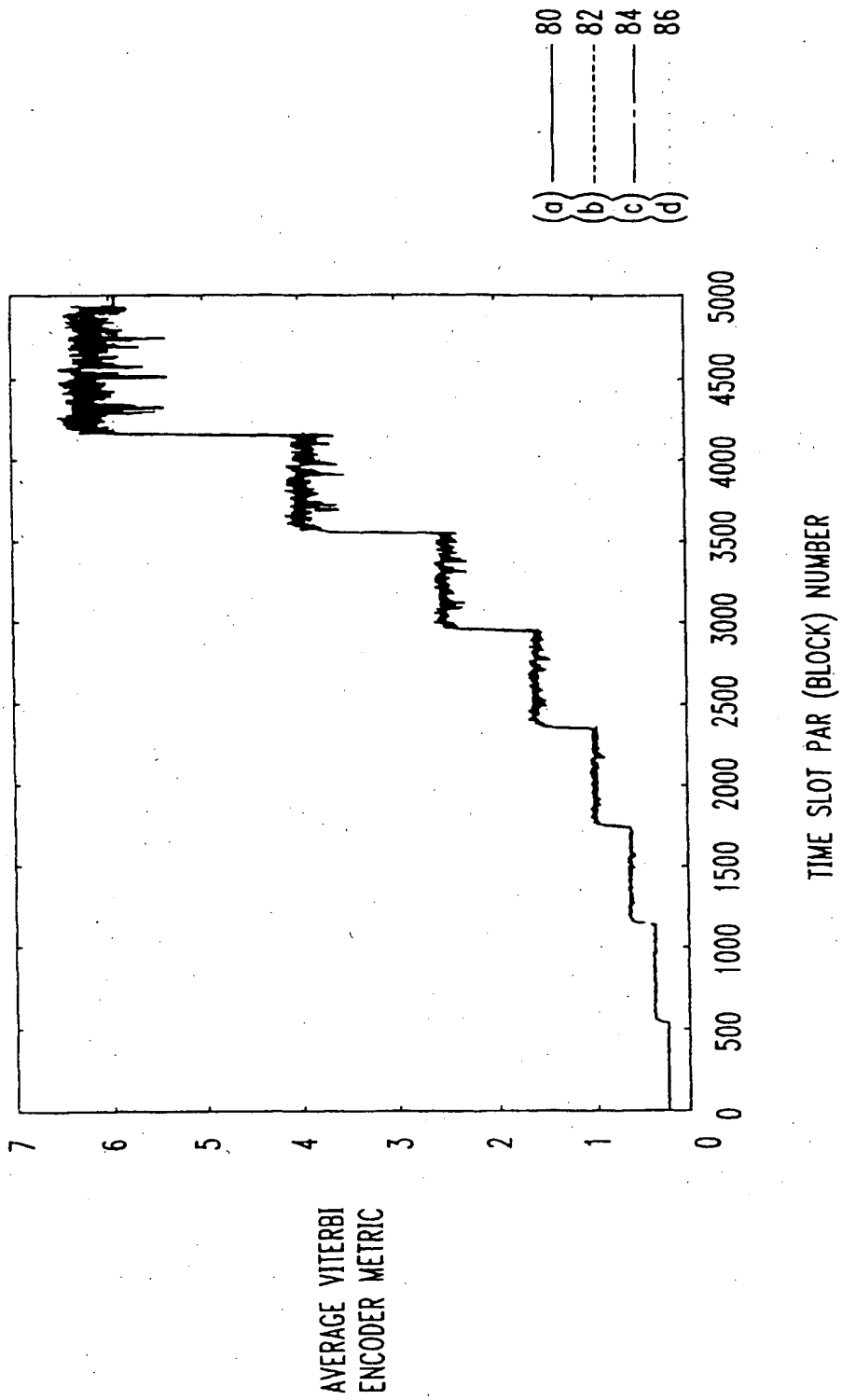

FIG. 5

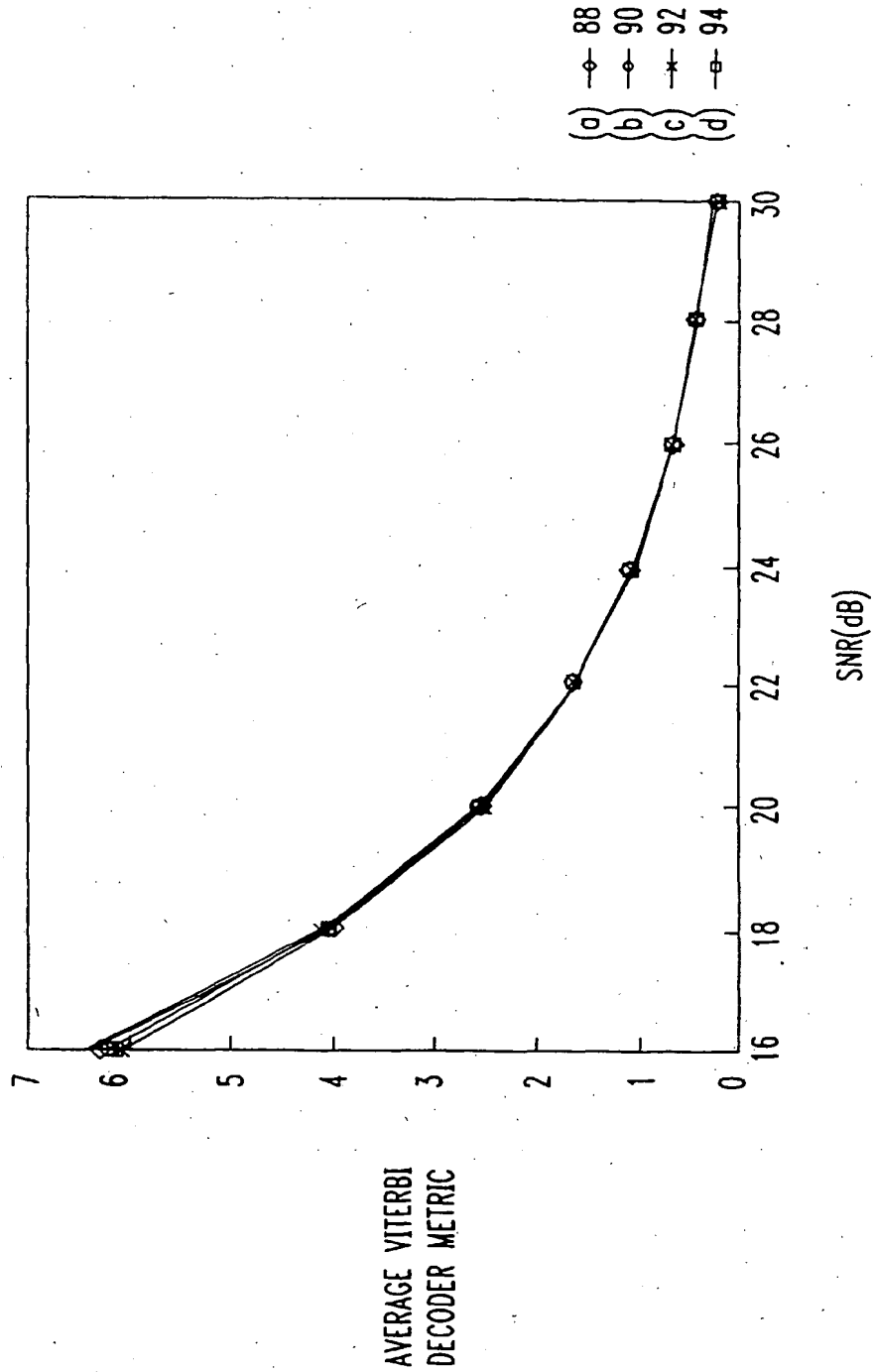

FIG. 6

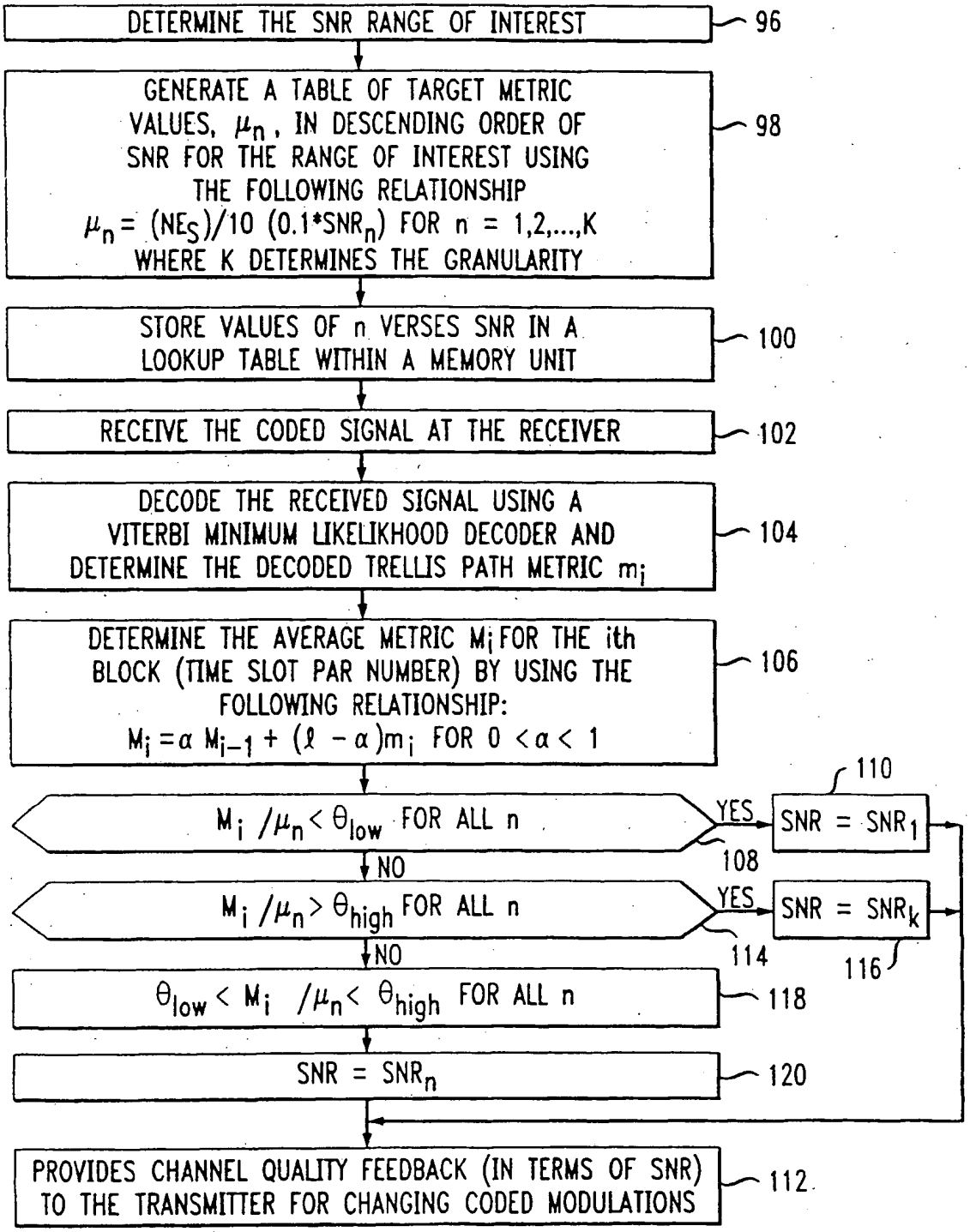

FIG. 7

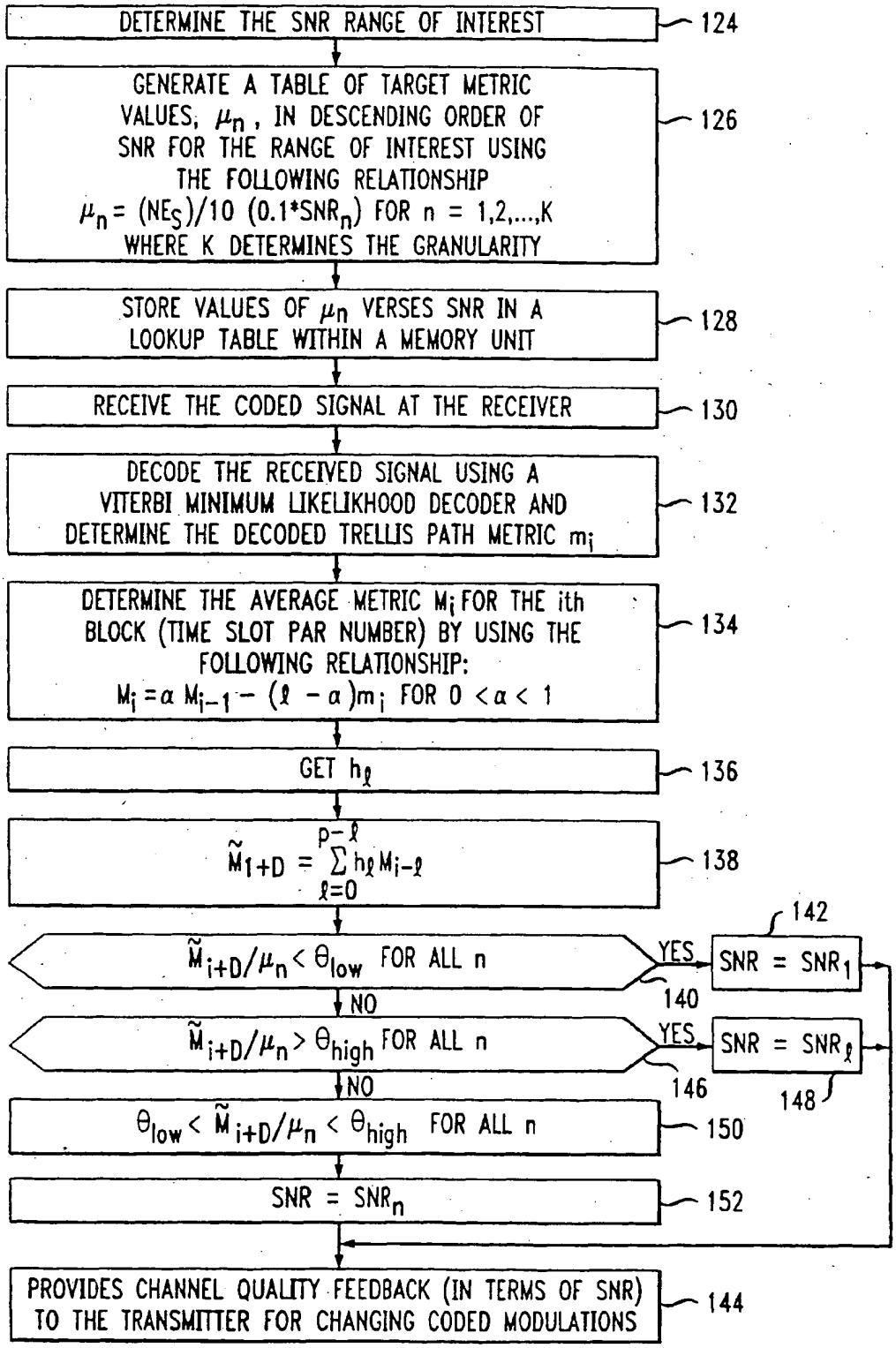

FIG. 8

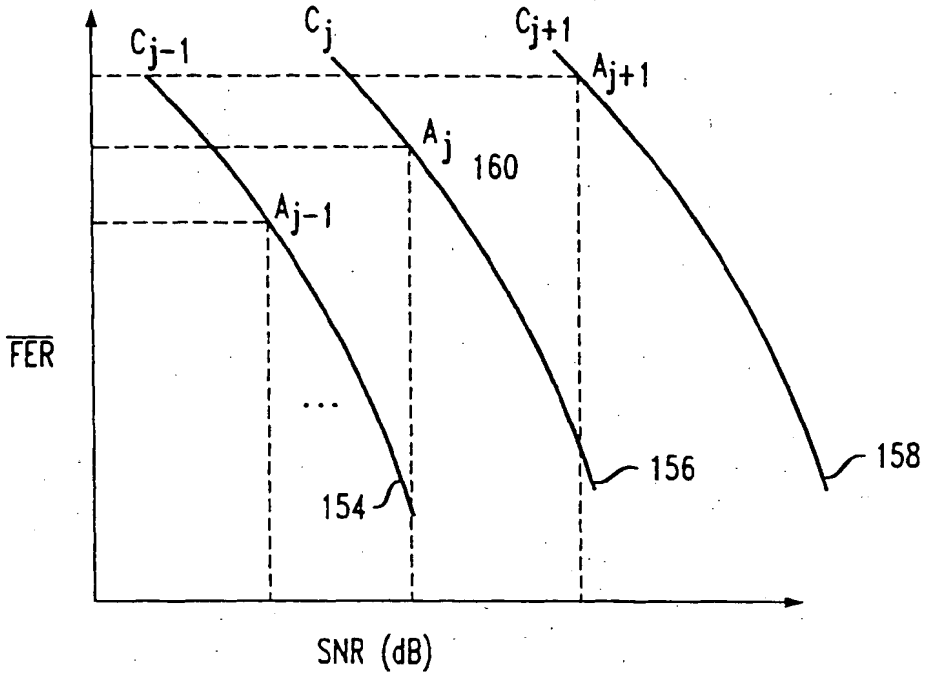

FIG. 9

CURRENT SCHEME	CONDITIONS ON METRIC	NEW SCHEME
C_1 C_2	$M_i/\mu_2 < \theta_{low}$	C_2
	$M_i/\mu_3 > \theta_{high}$	C_1
	$M_i/\mu_3 < \theta_{low}$	C_3
C_3	$M_i/\mu_3 > \theta_{high}$	C_2

FIG. 10

CURRENT SCHEME	CONDITIONS ON METRIC	NEW SCHEME
C_1	$M_i/\mu_3 < \theta_{low}$	C_3
C_2	$M_i/\mu_2 > \theta_{high}$	C_1
	$M_i/\mu_3 < \theta_{low}$	C_3
C_3	$M_i/\mu_3 > \theta_{high}$	C_2

FIG. 11

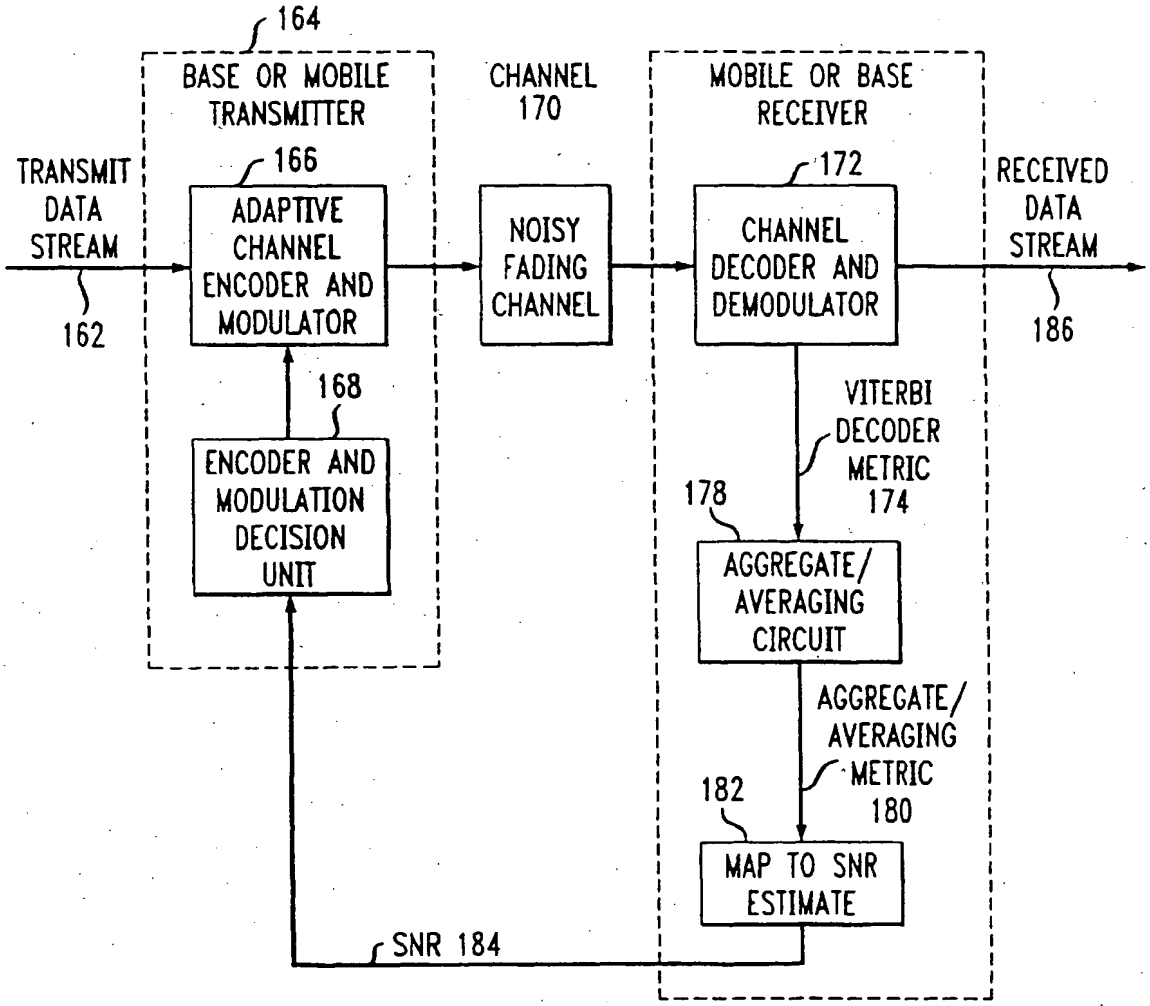

FIG. 12

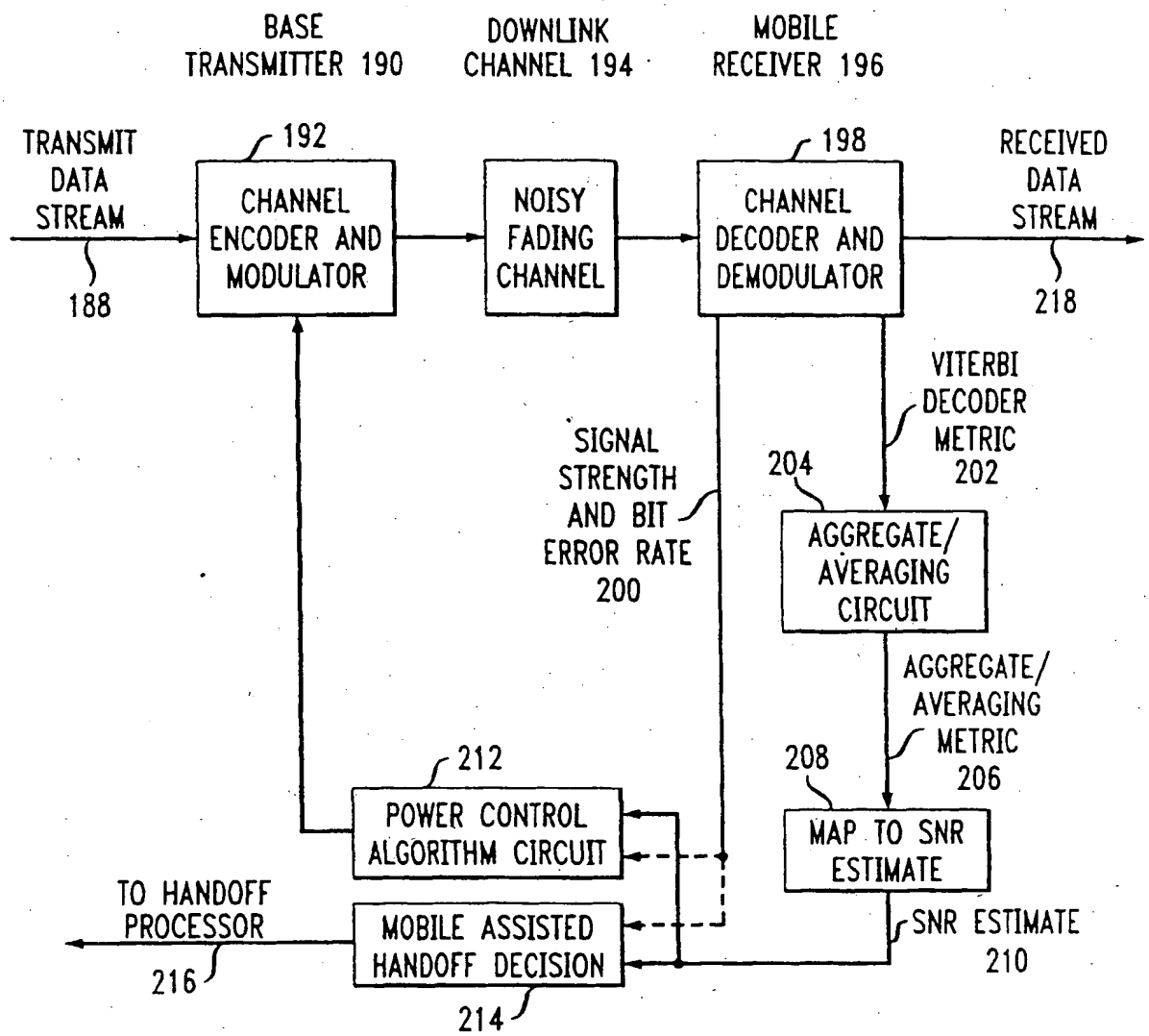
BASE TRANSMITTER 190
DOWNLINK CHANNEL 194
MOBILE RECEIVER 196
TRANSMIT DATA STREAM
188
192
CHANNEL ENCODER AND MODULATOR
NOISY FADING CHANNEL
198
CHANNEL DECODER AND DEMODULATOR
RECEIVED DATA STREAM
218
VITERBI DECODER METRIC 202
SIGNAL STRENGTH AND BIT ERROR RATE 200
204
AGGREGATE/ AVERAGING CIRCUIT
AGGREGATE/ AVERAGING METRIC 206
208
MAP TO SNR ESTIMATE
SNR ESTIMATE 210
212
POWER CONTROL ALGORITHM CIRCUIT
TO HANDOFF PROCESSOR
216
MOBILE ASSISTED HANDOFF DECISION
214

(19) Europäisches Patentamt
European Patent Office
Office européen des brevets

(11) EP 0 952 711 A2

EUROPEAN PATENT APPLICATION

(12)

(51) Int Cl.6: H04L 25/02

(43) Date of publication:
27.10.1999 Bulletin 1999/43

(21) Application number: 99302860.4

(22) Date of filing: 13.04.1999

(84) Designated Contracting States:
AT BE CH CY DE DK ES FI FR GB GR IE IT LI LU MC NL PT SE
Designated Extension States:
AL LT LV MK RO SI

(30) Priority: 23.04.1998 US 65193

(71) Applicant: LUCENT TECHNOLOGIES INC.
Murray Hill, New Jersey 07974-0636 (US)

(72) Inventors:
- Chen, Jiunn-Tsair
New Brunswick, New Jersey 08901 (US)
- Tsai, Huan-Shang
Whippany N.J. 07981 (US)
- Chen, Young-Kai
Berkeley Heights, New Jersey 07922 (US)

(74) Representative:
Buckley, Christopher Simon Thirsk et al
Lucent Technologies (UK) Ltd,
5 Mornington Road
Woodford Green, Essex IG8 0TU (GB)

(54) Joint maximum likelihood sequence estimator with dynamic channel description

(57) A cellular communication signal receiver (10) receives a desired signal in the presence of at least one co-channel interference signal. The receiver comprises a channel estimator (12) configured to receive a plurality of training signal samples to estimate the finite impulse response to the desired signal and the co-channel interference signal. The finite impulse response estimates having a predetermined number of channel taps define the length of the desired channel and the length of co-channel interference channel. A Viterbi decoder (20) is coupled to the channel estimator, and configured to receive the desired and co-channel interference signals. The channel estimator generates channel tap estimates.

A power calculator (14) is coupled to the channel estimator and configured to estimate the power of the estimated channel taps. A joint channel trimmer (18) is coupled to the power calculator and configured to maintain ajoint channel length, such that the desired signal channel length plus the co-channel interference channel length have a fixed size that defines the number of states the Viterbi decoder allocates to the desired signal and the co-channel interference signal.

FIG. 1

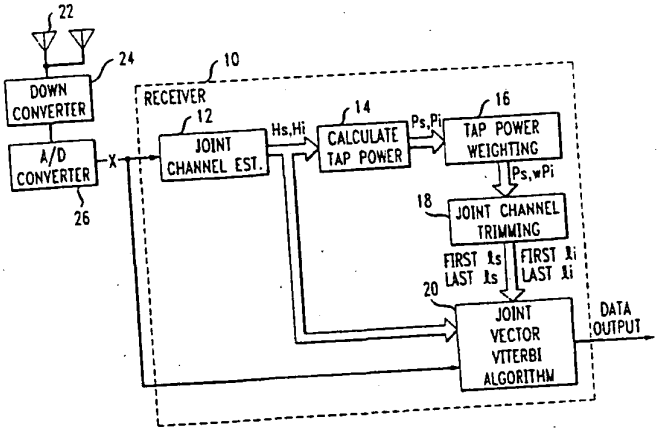

EP 0 952 711 A2

Printed by Jouve, 75001 PARIS (FR)

Description

Field Of The Invention

[0001] This invention relates to a cellular communication system and more specifically to a receiver system that is employed to receive digitally modulated signals in the presence of another modulated co-channel interfering (CCI) signal.

Background Of The Invention

[0002] In mobile radio communications, the radio spectrum is a scarce resource. As a result most mobile radio communications system are based on the cellular principle. Basically, a geographical area, within which wireless service is available, is divided into several cells. Schematically, each cell is represented as a hexagon; in practice, however, each cell has a shape that is dependent on, among other things, the topography of the terrain serviced by the system. Each cell includes a base station, which may be located approximately at its center. Each base station is configured to transmit and receive signals within approximately the area defined by each cell. However, the actual radio range of each base station may extend beyond each cell area. Therefore, it is desired that a different set of frequencies be allocated to the adjacent cells to avoid interference. Subscribers located within each cell area communicate with other subscribers by using a wireless terminal (e.g., a cellular telephone, a wireless local loop terminal, some cordless telephones, one-way and two-way pagers, PCS terminals and personal digital assistants). Each wireless terminal located within a cell sends to and receives signals from the corresponding base station located in that cell, over a communications channel within a predetermined frequency range.

[0003] Since adjacent cells employ different sets of frequencies, the distance between two cells that use the same frequency set may be an important design consideration. This distance is called the mean reuse distance *D*. In order to increase the total number of channels available per unit area, it is desired to decrease the size of the cells. By reducing the size of the cells, it is possible to reuse the same frequency sets more often. Thus, more subscribers may be able to use the system, because of the increase of available frequency sets within a predetermined area. However, depending upon the size of each cell, the transmission power of the base stations and the mobile units, severe co-channel interference between the cells that use the same frequency range may occur.

[0004] The maximum likelihood sequential estimation (MLSE) equalizer can equalize the channel at the receiver to achieve optimal performance. The MLSE equalizer is particularly useful in a radio channel with a long spread such as the one that employs a standard specification known as Global System for Mobile Communications (GSM). Another approach to reduce co-channel interference is to employ antenna arrays. Because of the frequent spatial separation between the desired signal and the co-channel interference signals, antenna arrays can suppress co-channel interference signals through beam forming. However, these approaches require very complicated signal processing in order to produce optimal results.

[0005] Thus, there is a need to reduce the complexity of such systems, to make them commercially feasible, and to reduce the effects of co-channel interference signals considerably.

Summary Of The Invention

[0006] In accordance with one embodiment of the invention, a communication signal receiver includes a channel estimator that is configured to receive a plurality of training signal samples to estimate the finite impulse responses to both desired signals and co-channel interference signals. These finite impulse response estimates have a predetermined number of channel taps defining desired channel length and the co-channel interference channel length respectively. The channel tap estimates are then provided to a Viterbi decoder. The channel tap estimates are also provided to a power calculator that estimates the power of each of the estimated channel taps. The individual tap power estimates are then provided to a joint channel trimmer. The joint channel trimmer maintains a joint channel length, such that the desired signal channel length plus the co-channel interference channel length have a fixed size, by truncating the weakest taps from both edges of the channel taps. The joint channel length is dynamically allocated between the desired channel taps and co-channel interference channel taps. The trimmed channel sizes are then provided to the Viterbi decoder, which decodes the received signals in accordance with the channel estimates and the calculated channel sizes.

Brief Description Of The Drawings

[0007] The subject matter regarded as the invention is particularly pointed out and distinctly claimed in the concluding portion of the specification. The invention, however, both as to organization and method of operation, together with

features, objects, and advantages thereof may best be understood by reference to the following detailed description when read with the accompanying drawings in which:

[0008] Fig. 1 illustrates a block diagram of a receiver in accordance with one embodiment of the present invention.

[0009] Fig. 2 illustrates a burst signal received by the receiver in accordance with one embodiment of the present invention.

[0010] Fig. 3 is a flow chart illustrating the operation process of a system in accordance with one embodiment of the present invention.

[0011] Fig. 4 illustrates a trellis diagram employed by a Viterbi decoder in accordance with one embodiment of the invention.

Detailed Description of The Drawings

[0012] Fig. 1 is a block diagram of a communications receiver in accordance with one embodiment of the invention, although the invention is not limited in scope in that respect. Receiver 10 includes a joint channel estimator 12 which is configured to receive signal samples *X* from an analog to digital A/D converter 26. These signal samples are digitized version of signals that have been received by an antenna array 22 and down converted to baseband by a down converter 24.

[0013] Antenna array 22 receives both desired signals within a cell and co-channel interference signals from locations outside a cell. Joint channel estimator 12 is configured to jointly estimate the finite impulse responses of the channels for both the desired signal and the co-channel interference signal.

[0014] Several approaches are being employed with respect to signaling standards for digital cellular telephone worldwide. One such standard is Europe's global system for mobile communications (GSM), described in ETSI/GSM Series 03 Air Interference Specification, GSM PN Paris, herein incorporated by reference. One aspect of the standard involves the transmission of signals in the form of signal bursts.

[0015] Fig. 2 illustrates a signal burst also known as a transmission burst or a signal frame, such as may be employed in a time division multiple access (TDMA) wireless communication system, although the invention is not limited in scope to a signal burst having this particular form or format. In the present context, the terms signal burst, transmission burst or signal frame may be used interchangeably. The signal or transmission burst illustrated in Fig. 2 has a predetermined number of digital symbols or bits. In this particular embodiment, each burst includes, in succession, a series of successive predetermined starting bits 27, a predetermined number of information bits 29, a series of predetermined training bits 31, a second predetermined number of information bits 33, and a series of successive predetermined ending bits 35. In GSM systems, for example, there are three starting and three ending bits, 57 bits in both portions of the signal burst comprising binary digital signals to be transmitted, and 26 training bits, referred to as the "midamble, " for a total of 148 bits per signal burst. The training bits are known at both the receiving and the transmitting end of the communications system. The starting and ending bits are likewise known and are typically "zeros." It will be appreciated that other numbers and distribution of bits are possible depending on the specification.

[0016] The GSM telecommunication standard requires a form of signal modulation in the baseband known as Gaussian Minimum Phase Shift Keying (GMSK). It is noted that although GMSK is not a linear modulation scheme it may be approximated as such. GMSK is described in more detail in Digital Phase Modulation, by J.B. Anderson, T. Aulin and C.E. Sundburg, 1986, available from Plenum, although, of course the invention is not limited in scope to GMSK modulation schemes.

[0017] Channel estimator 12 uses the training bits of an incoming burst as illustrated in Fig. 2, to calculate an estimate of the channels over which the transmission occurred. This channel estimate is the finite impulse response of the wireless channel through which the bursts are being transmitted from transmitter stations within a cell and outside a cell to a receiver station, such as receiver 10. The received signal is distorted due to noise and inter symbol interference (ISI) associated with transmission via the wireless channel. By minimizing the norm of the error signal, an estimate of the desired channel and co-channel interference channels is obtained. Each term in the impulse function is a complex quantity and is referred to in this context as a tap weight or channel tap. Each tap weight represents the effects of channel distortion on the transmitted signal, as will be explained in more detail below.

[0018] In order to obtain a channel estimate corresponding to both desired signals and co-channel interference signal, a channel model is employed as will be explained in more detail hereinafter.

[0019] Assuming a linear modulation scheme, the desired signal and the co-channel interference signal can be expressed respectively, as

$$\bar{s}(t) = \sum_{k} g_s(t-kT)s_k \qquad (1)$$

and

$$\bar{s}_i(t)=\sum_k g_{i,k}(t-kT)s_{i,k} \qquad (2)$$

where g_s, g_i are respectively, the pulse-shaping functions of the desired signal and co-channel interference signal. $\{s_k\}$, $\{s_{i,k}\}$ are, respectively, the data sequences of the desired signal and co-channel interference signal, and T is the period of each symbol or signal sample. Therefore, the signal received at the j^{th} antenna of antenna array 22 can be written as

$$x_j(t)=\int c_{sj}(t-\tau)\,\bar{s}(\tau)d\tau+\int c_{ij}(t-\tau)\,\bar{s}_i(\tau)d\tau+n(t) \qquad (3)$$

where $c_{s,j}(t)$ and $c_{i,j}(t)$ are respectively the physical channel impulse response of the j^{th} antenna of the desired signal and co-channel interference signal; and $n(t)$ is the additive noise. Substituting $\bar{s}(t)$ and $\bar{s}_i(t)$ from equations (1) and (2), equation (3) can be written as

$$x_j(t)=\sum_k s_k\ h_{s,j}(t-iT)\ +\sum_k s_{i,k}\ h_{i,j}(t-iT)\ +n(t) \qquad (4)$$

After sampling $x_j(t)$, equation (4) can be written in a matrix form as

$$X_{mxn}=(H_s)_{mxl}\,S_{lxn}+(H_i)_{mxl}\,(S_i)_{lxn}+N_{mxn} \qquad (5)$$

where the subscripts denote the size of the matrices; m is the number of antennas in antenna array 22; l is made long enough to cover all the non-zero terms of $h_{s,j}$ and $h_{s,d}$; n time samples are under consideration in equation (5); the i^{th} row of Hs is $[h_{s,j}(to), h_{s,j}(to-T),..., h_{s,j}(to-(l-1)T)]$ the i^{th} row of Hi is $[h_{i,j}(to), h_{i,j}(to-T),..., h_{i,j}(to-(l-1)T)]$; S is a Toeplitz matrix with $[s_k, s_{k-l}\,s_{k-l+1}]^T$ as its first column and $[s_k, s_{k+1}...s_{k+n-1}]$ as its first row; S_i is also a Toeplitz matrix with $[s_{i,k}, s_{i,k-l}, ...s_{i,k-l+1}]^T$ as its first column and $[s_{i,k}, s_{i,k+l}, ...s_{i,k+n-1}]$ as its first row.

[0020] Equation (5) can be written as

$$X=[Hs\ Hi]\begin{bmatrix}S\\S_i\end{bmatrix}+N \qquad (6)$$

wherein X refers to signal samples received by the receiver, and N is the additive noise received by the receiver. Assuming that noise N is a Gaussian white noise the least square solution can be written as

$$[Hs\ Hi]=\begin{bmatrix}S\\S_i\end{bmatrix}^+ \qquad (7)$$

where $(.)^+$ denotes pseudo-inverse, which is defined as $A^+ = (A^*A)^{-1}A^*$

[0021] It is noted that equation (7) provides the finite impulse response of the desired signal channel, H_s, and one co-channel interference channel H_i. However, there may be instances that more than one neighboring cell provides a co-channel interference signal. It is appreciated that equations (1) through (7) above may be expanded to incorporate additional co-channel interference signals. In that event, equation (7) may be expanded as

$$[Hs\ \ H_{i,1}....H_{i,n}]\cdot\ x\begin{bmatrix}S\\Si\\\cdot\\Sn\end{bmatrix}^{\cdot} \qquad (7a)$$

wherein $H_{i,n}$ corresponds to finite impulse response of the co-channel interference signal provided via the n^{th} channel from cell n proximate to the cell wherein the desired signal is transmitted and Sn is the training sequence provided by

the base station at cell *n*.

[0022] Thus, joint channel estimator 12 is configured to derive channel estimates based on training bits and actual received signal as shown in equations (7) or (7a).

[0023] The channel tap estimates are then provided to a Viterbi decoder 20 to demodulate both the desired signal and the co-channel interference signal. The channel tap estimates are also provided to an input port of a tap power calculator 14. The output port of tap power calculator 14 is coupled to an input port of a tap power weighing unit 16, which is configured to multiply the channel taps corresponding to the co-channel interference taps by a weighing factor. Thereafter the output port of tap power weighting unit 16 is coupled to a joint channel trimmer 18, which is configured to truncate a plurality of channel taps corresponding to the desired signal and the co-channel interference signal such that the total number of taps represeriting the channel estimates for both signals remain a constant, as will be explained in more detail hereinafter.

[0024] The output port of joint channel trimmer 18 is coupled to an input port of joint Viterbi decoder 20, which is configured to have a fixed number of states as set forth by the number of taps specified by channel trimmer 18.

[0025] Tap power calculator 14 is configured to calculate the strength of each finite impulse response tap for both the desired signal and the co-channel interference signal. The strengths of the finite impulse response taps for the desired signal channel is referred to as *Ps* and the finite impulse response taps for the co-channel interference signal channel is referred to as *Pi*. Thus power signal *Ps* and power signal *Pi* can be written as

$$P_s = 1_{lxm}(H_s \odot conj\,(H_s)),\ P_i = 1_{lxm}(H_i \odot conj\,(H_i)) \tag{8}$$

wherein 1_{lxm} is a column vector with each element being one, conj(.) denotes the complex conjugate operation and $\odot$ denotes the Hadamard product.

[0026] Fig. 3 is a flow chart illustrating the operation of receiver 10 in accordance with one embodiment of the invention, although the invention is not limited in scope in that respect. During operation, at step 110, joint channel estimator 12 for each received burst obtains a joint channel estimation for both desired signals and co-channel interference signals received by receiver 10. Joint channel estimator 12 employs the training bits in each burst to obtain the joint channel estimation for the desired signals and co-channel estimation signals as described above. To this end joint channel estimator 12 provides a plurality of channel taps corresponding to the desired and co-channel interference signals.

[0027] At step 112 tap power calculator 14 calculates the power *Ps* and *Pi* of the channel taps obtained at step 110, in accordance with equation (8) as described above. Thereafter, at step 114 tap power weighing unit 16 multiplies a weighing factor w with channel tap power values corresponding to co-channel interference signal so as to de-emphasize the effect of co-channel interference signals. This follows, because the data bits embedded in the co-channel interference signal are of no interest to receiver 10. Preferably, the weighing factor *w* is chosen to be close but less than one.

[0028] At step 116, joint channel trimmer 16 truncates the combined number of channel taps corresponding to the desired and co-channel interference signal to a fixed specifiable number, l_c. It is noted that a large value for l_c means relatively lower channel estimation error in the Viterbi decoder and relatively higher complexity. For example every unit increase to l_c leads to doubling the complexity of the Viterbi decoder employed in receiver 10.

[0029] Thus, joint channel trimmer 18 truncates the end portions of channel taps corresponding to both desired and co-channel interference channels by finding the weakest tap power based on

$$min\,\{\,P_s\,(l_{s,\,first}),\ P_s\,(l_{s,\,last}),\ wP_i\,(l_{i,\,first})\ wP_i\,(l_{i,\,last})\,\} \tag{9}$$

where $l_{s,\,first}$, $l_{s,\,last}$, $l_{i,first}$, $l_{i,last}$ are respectively the first and the last taps of the finite impulse response channel taps of the desired and co-channel interference signals with $l_{s,\,first} \geq l_{s,\,last}$ and $l_{i,first} \geq l_{i,\,last}$. Thus, channel trimmer 18 compares the power corresponding to the first and last channel taps and eliminates the tap with the weakest power. For example, if the power of the first channel tap $P_s\,(l_{s,first})$ is the weakest, it gets truncated by the channel trimmer. Similarly if the power of the last channel tap $_{ll}\,(l_{i,\,lsat})$ is the weakest tap, it gets truncated by the channel trimmer. Step 116 is repeated until channel trimmer 18 at step 118 determines that combined number of the remaining channel taps, i.e., $(l_{s,first} - l_{s,last}) + (l_{i,first} - l_{i,last}) = l_c$, wherein l_c is a fixed number. It is noted that the term $(l_{s,first} - l_{s,last})$ corresponds to the remaining number of channel taps, l_s, corresponding to the desired signal and $(l_{i,first} - l_{i,last})$ corresponds to the remaining number of channel taps, l_i, corresponding to the co-channel interference channel.

[0030] It is noted that for those bursts with a high carrier to interference ratio (CIR), the system employs all the taps to describe the desired signal channel to reach the lower bound of a bit error rate. Conversely, for those bursts with a lower carrier to interference ratio, the system employs more taps for the co-channel interference channel so as to

mitigate the impact of co-channel interference.

[0031] Once the channel taps corresponding to desired signal and co-channel interference signal is selected, Viterbi decoder 20 employs the remaining channel taps, indicated by $l_{s,first}$, $l_{s,last}$, $l_{i,first}$, and $l_{i,last}$ l_s and l_i to decode the signals X that are provided from antenna array 22.

[0032] Thus, at step 120, Viterbi decoder 20 demodulates both the desired data sequences and co-channel interference data sequences. Viterbi decoder 20 is a maximum likelihood decoder that provides forward error correction. The Viterbi decoder works back through a sequence of possible bit sequences at each symbol instant to determine which bit sequences are more likely to have been transmitted. The possible transitions from a signal status at one symbol instant, or state, to a signal status at a subsequent, symbol instant or state is limited. Each possible transition from one state to a next state may be illustrated graphically and is referred as a branch in this context. A sequence of interconnected branches is referred to as a path in this context. Each state may transition only to a limited number of next states upon receipt of the next bit (or set of bits) in the bit stream. Potential paths remain while other potential paths are eliminated during the decoding process. Thus by eliminating those paths that are not permissible, computational efficiency may be achieved in determining the most likely paths to have been transmitted.

[0033] In accordance with one embodiment of the invention, because channel taps corresponding to desired signal and co-channel interference signal are truncated on a burst-to-burst basis, the number of states in the Viterbi decoder that correspond to the desired signal and the co-channel interference signal may differ from one burst to the other. For example, in accordance with one embodiment of the invention, the total number of channel taps l_c may be 5, as illustrated in Fig. 4.

[0034] Thus, for an exemplary data burst, after channel truncation, channel trimmer 18 allocates three channel taps to the desired channel and two channel taps to co-channel interference channel. As illustrated in Fig. 4, Viterbi decoder 20 operates with an 8-state trellis 210 that correspond to the 3-tap channel memory corresponding to the desired channel, and with a 4-state trellis 212 that correspond to the 2-tap channel memory corresponding to the co-channel interference channel. Thus, as illustrated in Fig. 4, each branch in 8-state trellis 210 is expanded to 4-state trellis 212. The total number of states is the product of the numbers of the desired signal states and the co-channel interference states. Thus, for the example illustrated in Fig. 4, the total number of states is 32. Each state has four input branches and four output branches.

[0035] At step 122, the Viterbi decoder decodes the received signal. For each branch, Viterbi decoder 20 reconstructs the received signal $\bar{x}$. Viterbi decoder 20 then employs the Fobenius norm square of the difference between the reconstructed received signal and the actual received signal, $\| \bar{X} - X \|^2_F$, as the incremental metrics for each branch, wherein the operator $\|\cdot\|_F$, denotes the Fobenius norm. By minimizing the node metric in the Viterbi algorithm, Viterbi decoder 20, searches for the most likely data sequence in the trellis.

[0036] Once the data for one burst is estimated, step 110 is repeated again for following bursts.

[0037] Thus, in accordance with the present invention, a wireless receiver is able to receive signals with substantially low bit error rates. Furthermore, features such as weighing the channel power taps corresponding to co-channel interference signals, and truncating the total number of channel taps allow for a relatively simple and inexpensive arrangement.

[0038] While only certain features of the invention have been illustrated and described herein, many modifications, substitutions, changes or equivalents will now occur to those skilled in the art. It is therefore, to be understood that the appended claims are intended to cover all such modifications and changes that fall within the true spirit of the invention.

Claims

1. A cellular communication signal receiver for receiving a desired signal in the presence of at least one co-channel interference signal, said receiver comprises:

   a channel estimator configured to receive a plurality of training signal samples to estimate the finite impulse response to said desired signal and said co-channel interference signal, said finite impulse response estimates having a predetermined number of channel taps defining the length of the desired channel and the length of co-channel interference channel;

   a Viterbi decoder coupled to said channel estimator and configured to receive said desired and co-channel interference signals, and said channel tap estimates generated by said channel estimator;

   a power calculator coupled to said channel estimator and configured to estimate the power of said estimated channel taps;

   a joint channel trimmer coupled to said power calculator and configured to maintain a joint channel length, such that the desired signal channel length plus the co-channel interference channel length have a fixed size that defines the number of states said Viterbi decoder allocates to said desired signal and said co-channel

interference signal.

2. The receiver in accordance with claim 1, wherein signals received by said receiver are formatted as signal bursts, and said channel estimator estimates said channels on a burst-by-burst basis.

3. The receiver in accordance with claim 2, wherein said joint channel trimmer is coupled to said Viterbi decoder.

4. The receiver in accordance with claim 3, further comprising a power weighing unit coupled to said tap power calculator configured to multiply said estimated channel taps corresponding to co-channel interference signal by a weighing factor.

5. The receiver in accordance with claim 4, wherein said weighing factor is less than one and said power weighing unit is coupled to said joint channel trimmer.

6. The receiver in accordance with claim 5, wherein said channel trimmer dynamically allocates said fixed channel length between the desired channel taps and co-channel interference channel taps.

7. A method for receiving a desired signal in the presence of at least one co-channel interference signal, said method comprising the steps of:

(a) receiving a plurality of training signal samples ;
(b) in response to said signal samples estimating the finite impulse response of channels corresponding to said desired signal and said co-channel interference signal, by generating a predetermined number of channel taps defining the length of the desired channel and the length of co-channel interference channel;
(c) calculating the power corresponding to each one of said estimated channel taps;
(d) trimming said channel taps so as to maintain a joint channel length, such that the desired signal channel length plus the co-channel interference channel length have a fixed size; and
(e) decoding signals received by said receiver by employing said trimmed channel taps.

8. The method in accordance with claim 7, further comprising the step of repeating steps (a) through (e) on a burst by burst basis.

9. The method in accordance with claim receiver in accordance with claim 8, wherein said decoding step comprises the step of Viterbi decoding said received signals.

10. The method in accordance with claim 9, further comprising the step of multiplying said estimated channel taps corresponding to co-channel interference signal by a weighing factor.

11. The method in accordance with claim 10 comprising the step of setting sad weighing factor to a number less than one.

12. The method in accordance with claim 10, wherein said trimming step further comprises the step of dynamically allocating said fixed joint channel length between the desired channel taps and co-channel interference channel taps, on a burst-by-burst basis.

FIG. 1

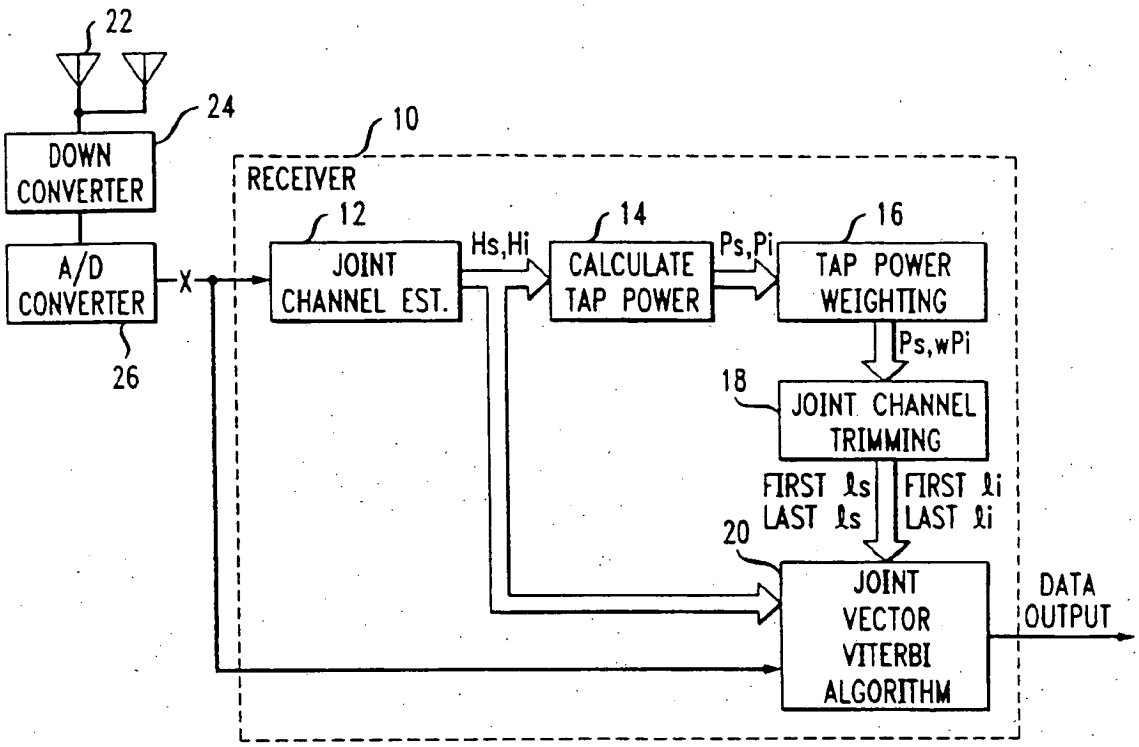

FIG. 2

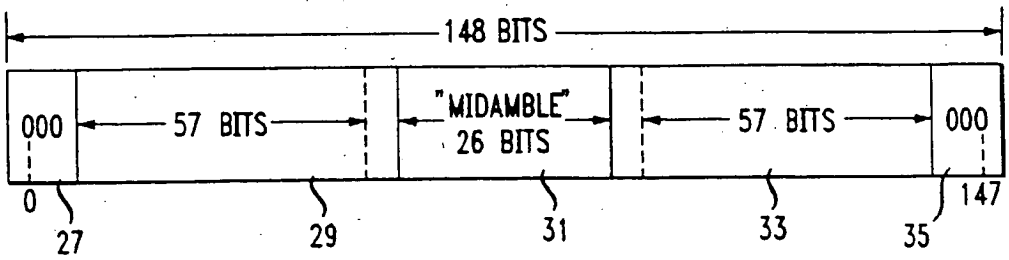

FIG. 3

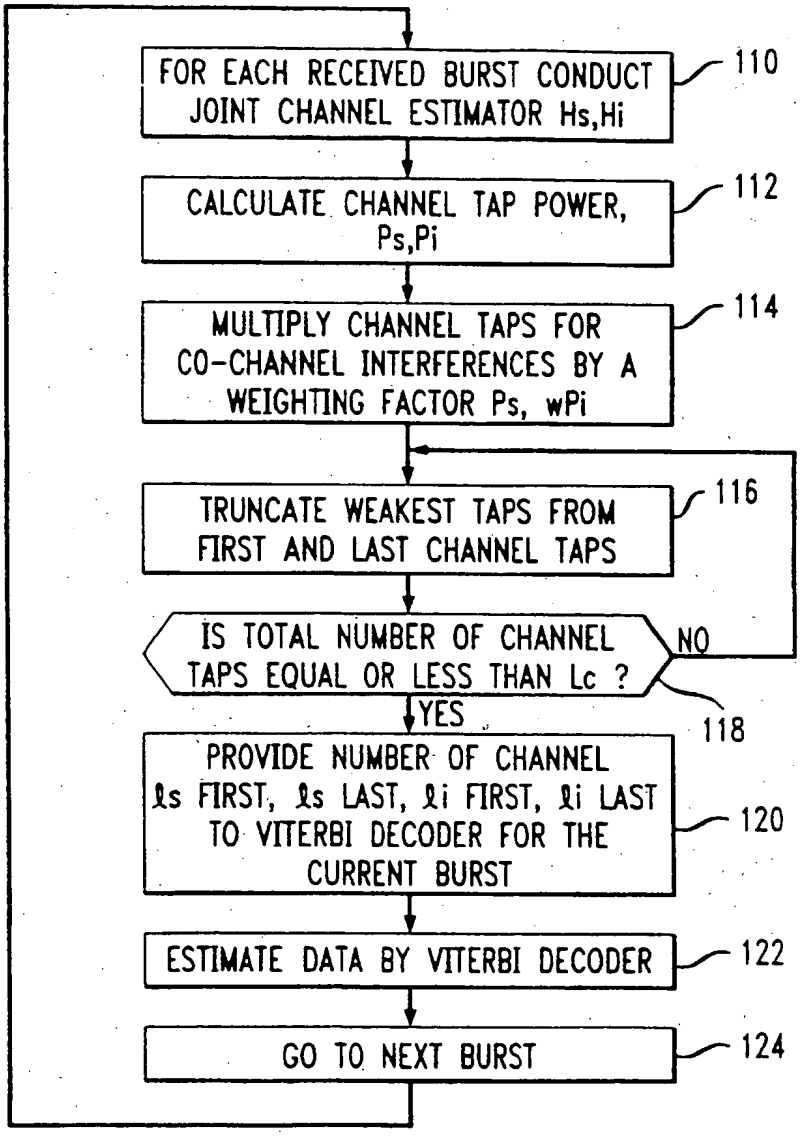
FOR EACH RECEIVED BURST CONDUCT JOINT CHANNEL ESTIMATOR Hs,Hi
110
CALCULATE CHANNEL TAP POWER, Ps,Pi
112
MULTIPLY CHANNEL TAPS FOR CO-CHANNEL INTERFERENCES BY A WEIGHTING FACTOR Ps, wPi
114
TRUNCATE WEAKEST TAPS FROM FIRST AND LAST CHANNEL TAPS
116
IS TOTAL NUMBER OF CHANNEL TAPS EQUAL OR LESS THAN Lc ?
NO
YES
118
PROVIDE NUMBER OF CHANNEL ℓs FIRST, ℓs LAST, ℓi FIRST, ℓi LAST TO VITERBI DECODER FOR THE CURRENT BURST
120
ESTIMATE DATA BY VITERBI DECODER
122
GO TO NEXT BURST
124

FIG. 4